


Effect of aging on the properties of TiO₂ nanoparticle

Nafise Ebrahim Jasbi¹ · Davoud Dorrnanian² 

Received: 28 December 2015 / Accepted: 9 February 2016 / Published online: 20 February 2016
© The Author(s) 2016. This article is published with open access at Springerlink.com

Abstract Effect of aging on the properties of titanium dioxide nanoparticles produced by laser ablation process in water is investigated experimentally. The fundamental wavelength of a Q-switched Nd:YAG laser was employed to irradiate a high-purity Ti plate in distilled water at temperatures of 20, 35, 50 and 65 °C. Produced nanoparticles were diagnosed by UV–Vis–NIR spectroscopy, X-ray diffraction method, and dynamic light scattering device immediately after production and 1 week after. Bandgap energy of samples was extracted using Tauc method. Size of nanoparticles was increased after a week and their bandgap energy was decreased. Results show that the phase of TiO₂ nanoparticles was transited from brookite to rutile after 1 week.

Keywords Laser ablation · TiO₂ nanoparticle · Absorption spectra · XRD · Excitonic resonance

Introduction

Optical properties of materials such as thin films and nanostructures have been at the focus of many researchers in the last decade. Among them diamond like carbon, zinc oxide and titanium oxide thin films were more applicable than others [1–5].

Recently, utilization of TiO₂ nanocrystals in optical, electrical, photocatalytic and pigment has received considerable attention. Superior physicochemical behavior, relatively low cost and easy handling are some of their advantages. TiO₂ properties are strongly related to phase structure, morphology and particle size distribution. TiO₂ photocatalytic performance is especially critically affected by its particle size. The monodisperse TiO₂ nanoparticles also exhibit photocatalytic effect. Titanium dioxide has three principal crystallographic structures called anatase (tetragonal), rutile (tetragonal) and brookite (orthorhombic) [6–10]. The most stable phase is rutile, whereas anatase is a metastable phase at ambient temperature. The photo-activity of the latter is at the same time generally superior to that of the former. High-temperature photocatalysis applications of TiO₂ nanoparticles demand, therefore, anatase thermal stability not to convert into the rutile phase. Aging sometimes leads to phase change of TiO₂ nanoparticles spontaneously. To control the process we have to study several features of aging on the structure of TiO₂ nanoparticles.

Aging is the operation often uses in the synthesis of nanoparticles. It sometimes causes macroscopic or microscopic changes in the solid phase, especially modification of crystal type and size, specific surface changes or changing in chemical composition of solid phase, and it is commonly a slow process. Aging temperature is an important parameter in the phase transition of TiO₂ NPs due to aging. So that aging for 6 h at temperature below of 70 °C leads to the formation of rutile crystalline phase and at temperature higher than 70 °C leads to the formation of anatase crystalline phase. Increasing of aging time at a specific temperature leads to increasing conversion phase and crystal size [11, 12]. Mahoney et al. reported on the effect of aging time on the evolution of TiO₂ NPs using

✉ Davoud Dorrnanian
dorand@sbiau.ac.ir

¹ Physics Department, Science Faculty, Central Tehran Branch, Islamic Azad University, Tehran, Iran

² Laser Laboratory, Plasma Physics Research Center, Science and Research Branch, Islamic Azad University, Tehran, Iran

TEM micrographs, XRD pattern, and Raman spectra of samples [13]. In their experiments it took about 6 days for anatase nanoparticles to change to rutile type.

Effects of 1 week aging at room temperature on the nature of TiO₂ nanoparticles produced by laser ablation in water at different temperatures have been studied experimentally in this manuscript. Results confirm the phase transition of NPs from brookite phase to rutile first.

Experimental setup

TiO₂ NPs were produced by pulsed laser ablation of a high-purity Ti plate in deionized water. A titanium plate was placed on the bottom of an open glass cylindrical vessel filled with 35 ml deionized water. Height of water on the target was 2 cm. The Ti plate and containers were cleaned ultrasonically in alcohol, acetone and deionized water before the experiments. Ti plate was irradiated with 5000 pulses of a Nd:YAG laser operated at 10 Hz repetition rate with 6 ns pulse width. TiO₂ NPs were produced using the 1064 nm wavelength of laser at 2 J/cm² fluence. The diameter of the output pulse of laser was 6 mm which was focused with 80 mm focal length lens on the surface of the target in water. The spot size of laser pulse on the target surface was calculated to be about 30 μm. Temperature of water in the ablation experiment was 20, 35, 50, and 65 °C for samples 1–4, respectively. Details of the effect of water temperature on the properties of nanoparticles were reported elsewhere [14]. Absorption and transmission spectrum of samples, their size distribution, and lattice structure were recorded after production of nanoparticles, and 1 week after production.

The optical properties of the nanoparticle solution were examined at room temperature by a UV–Vis–NIR absorption spectrophotometer PG instruments (T80) and Dynamic light scattering (DLS) measurement was done using the Nano ZS (red badge) ZEN 3600 device from Malvern Co, for studying the size distribution of the nanoparticles in water. Normally, 500 or more particles were counted to determine the size distribution of each sample. The crystalline structure of the samples was analyzed by X-ray diffraction (XRD) of dried suspensions on Si substrate, with Cu-K α radiation ($\lambda = 1.54060 \text{ \AA}$), using an X'Pert MPD diffractometer from Phillips company.

Results and discussion

Pictures of nanoparticle suspension in water are shown in Fig. 1. After ablation the color of samples was light blue (Fig. 1a), but after a week they were almost colorless (Fig. 1b). The same result was observed by Singh et al.

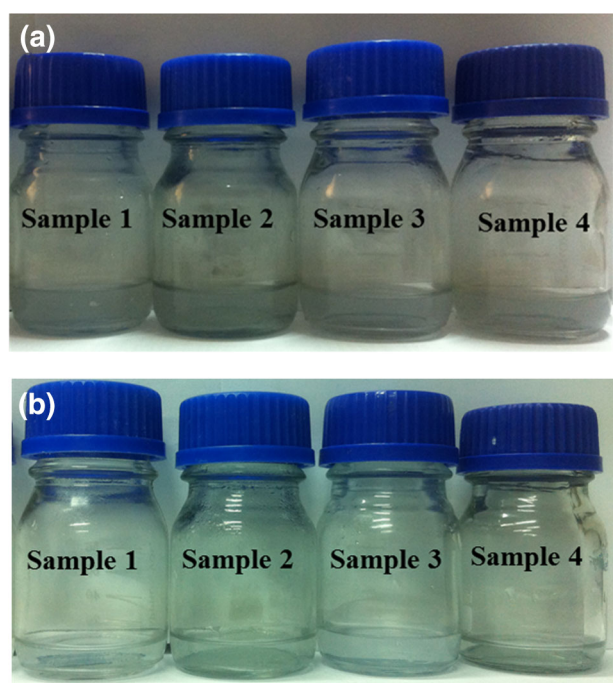


Fig. 1 Pictures of colloidal nanoparticles prepared by nanosecond laser ablation of titanium in **a** after ablation, **b** 1 week after ablation

[15]. The color of nanoparticles depends on their size. According to literature with increasing size of TiO₂ nanoparticles their color gradually changes from light blue to colorless [15].

UV–Vis–NIR spectrum of samples are shown in Fig. 2a and b. Figure 2a shows the spectrum of samples exactly after ablation. The excitonic peak of TiO₂ NPs occurs at $\lambda < 200 \text{ nm}$ at that time. While after 1 week the excitonic absorption peak of NPs was shifted to about 300 nm. This large red shift of excitonic absorption peak of samples may be due to their size enlargement of more than 50 nm. It also can be due to increase in the oxidation of Ti nanoparticles. Another reason for red shifting of the excitonic peak of NPs is their phase transition. $\lambda < 200 \text{ nm}$ is the wavelength that corresponds to the excitonic absorption peak of metastable TiO₂ nanoparticles, while after a week these peaks were shifted to around 300 nm which is the wavelength corresponding to excitonic absorption of rutile TiO₂ nanoparticles [16]. According to the results, the phase of TiO₂ nanoparticles was changed from metastable phase to rutile stable phase in a week. Absorption spectra of NPs were checked after 2 weeks. Peaks were fixed at 300 nm, showing that the rutile phase of TiO₂ NPs is the stable phase.

The absorption coefficient spectra of particles versus photon energy are plotted in Fig. 3a after ablation and Fig. 3b 1 week after ablation. They are extracted from transmission spectra of samples employing Beer–Lambert law:

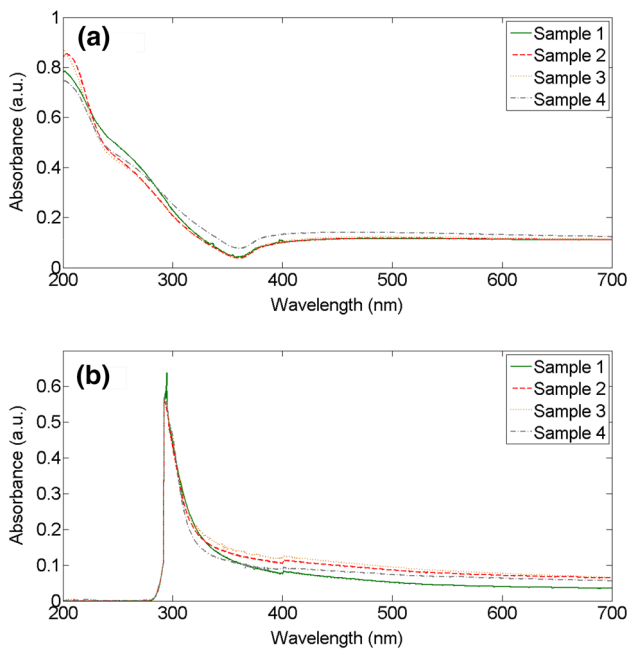


Fig. 2 The UV–Vis–NIR absorption spectrum of samples **a** immediately after ablation, **b** 1 week after ablation

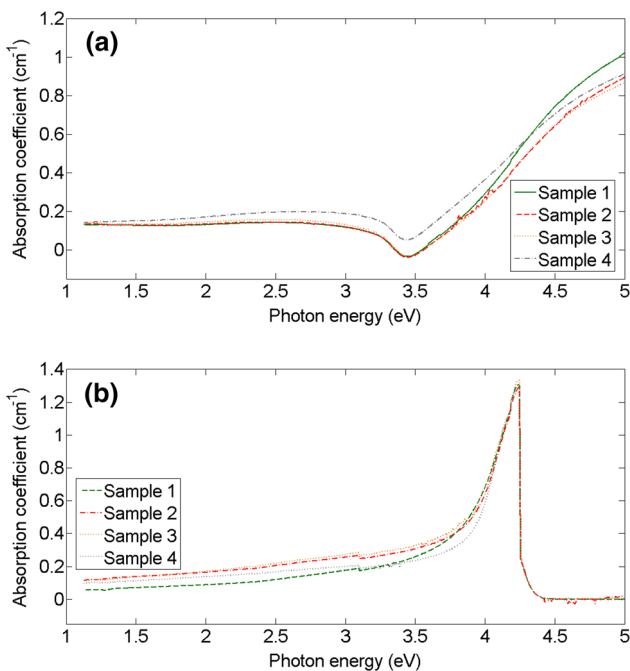


Fig. 3 The absorption coefficient of TiO₂ NPs **a** after ablation, **b** 1 week after ablation

$$\alpha = -\ln(T)/d \tag{1}$$

in which α is the absorption coefficient, T is transmission with distilled water as the reference, and d is the thickness of sample. The thickness of samples was taken equal to

coverts thickness which was 10 mm. There is no noticeable difference between them. They show the typical behavior of a semiconductor absorption coefficient. Before aging, there is an excitonic absorption peak at 4 eV. The absorption edge is very sharp due to large bandgap energy of samples. After a week the absorption peak was shifted to >5 eV. Decreasing the slope of absorption edge confirms that the energy gap was decreased after a week. Results show large differences of optical behavior of TiO₂ nanoparticles due to aging.

The optical bandgap energy of samples is also determined from their absorption spectrum using Tauc method [17, 18]. In this method the absorption spectrum of semiconductors and insulators at the absorption edge obey the equation

$$(\alpha h\nu) = B(h\nu - E_g)^m \tag{2}$$

where B is a constant magnitude, h is the Planck constant, ν is the probe radiation frequency, and E_g is the optical bandgap energy. Depending on direct or indirect allowed transition m is 1/2 or 2, respectively. According to Tauc method the absorption edge in $(\alpha h\nu)^{1/m} - h\nu$ plot is a line which intersects the $h\nu$ axis at E_g . Taking $m = 2$, for the indirect allowed transition, the optical bandgap energy of samples are extracted and presented in Table 1. Increasing the water temperature led to decrease the bandgap energy of nanoparticles from sample 1–4. It showed that the size of nanoparticles was increased with increasing temperature the water. From another side of view aging also decreased the bandgap energy of nanoparticles. It may be due to two phenomena: one is size enlargement and another is phase transition. After a week size of nanoparticles was increased because the rutile TiO₂ NPs are larger than brookite and rutile ones [19].

The X-ray diffraction patterns of samples are shown in Fig. 4a and b. X-ray diffraction measurement was performed for the dried film of samples from the concentrated suspension on a Si substrate. A peak of X-ray photons diffracted from Si substrate can be seen at $2\theta = 69.41^\circ$. The XRD spectrum clearly shows the mono crystalline structure of the nanoparticles. As shown in Fig. 5a, the existence of brookite in the XRD patterns is clearly evidenced from the presence of the (121) peak at the $2\theta = 33.05^\circ$ [20]. With increasing the temperature of water, (110) planes of rutile phase of TiO₂ are also formed

Table 1 The bandgap of energy for samples produced by PLA obtained after ablation and 1 week after ablation

Bandgap (eV)	Sample 1	Sample 2	Sample 3	Sample 4
After ablation	4.8	4.7	4.6	4.4
1 week after ablation	3.3	3.4	3.5	3.7

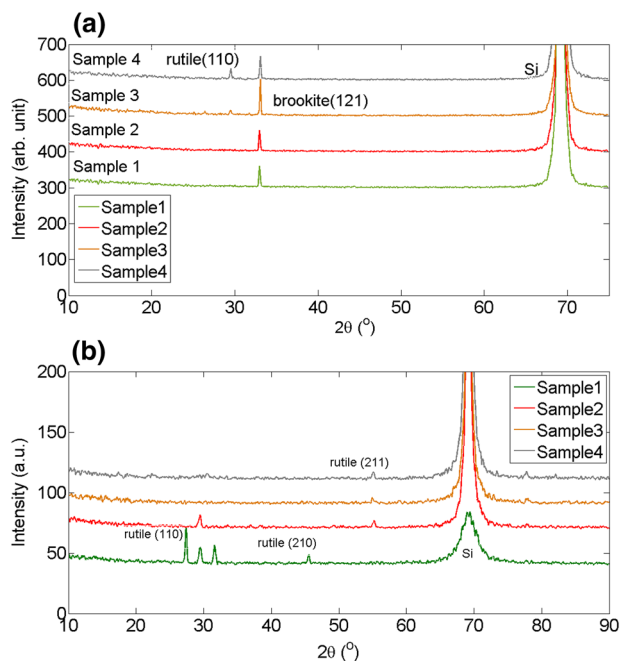


Fig. 4 X-ray diffraction pattern of TiO₂ nanoparticles prepared by pulsed laser ablation in deionized water **a** after ablation **b** 1 week after ablation

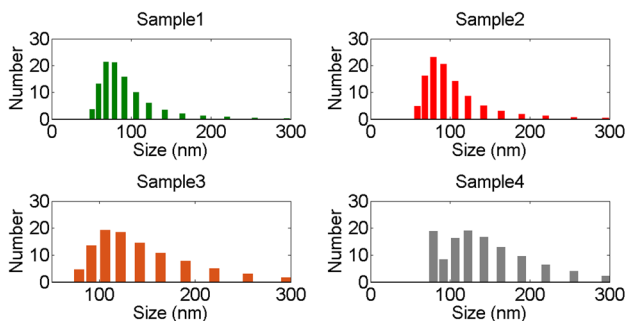


Fig. 5 Plots of size distribution TiO₂ NPs after ablation measured by the DLS method

at $2\theta = 29.48^\circ$. The peaks of the XRD pattern of samples were changed completely after a week. As is shown in Fig. 5b, all peaks are due to the formation of rutile structure of TiO₂ in samples. Increasing the temperature of ablation environment was led to formation of rutile phase of TiO₂ exactly after ablation but after a week we have only rutile phase of TiO₂ in the structure of samples. Rutile is the common structure of stable form of TiO₂. In other words, 1 week is enough for TiO₂ nanoparticle to reach to stable form. Shahini et al. reported on the phase change of TiO₂ nanopowder to anatase after 12 h [12].

Hydrodynamic size distribution of samples has been measured using the DLS method. That is one of the most reliable methods to measure the size distribution of

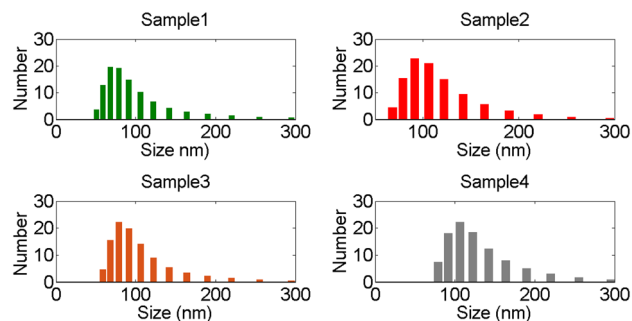


Fig. 6 Plots of size distribution TiO₂ NPs 1 week after ablation measured by the DLS method

nanoparticles. Hydrodynamic size of nanoparticles is their real diameter plus the diameter of the electrostatic potential around them, so it is larger than the real size of NPs. The plots of size distribution of samples are presented in Fig. 5 after ablation and Fig. 6 1 week after ablation. With aging, the hydrodynamic diameter of the nanoparticles was increased. Increasing the size of nanoparticles may be another reason for their phase transition from brookite to rutile phase. It is interesting to mention that rutile is the most stable phase for TiO₂ NPs. Anatase is the most stable phase for NPs below 11 nm and brookite has been found to be the most stable for NPs in the 11–35 nm range [19]. The results of DLS confirms that one of the mechanisms, responsible for decreasing the bandgap energy of nanoparticles is their size enlargement.

Conclusion

TiO₂ nanoparticles were prepared by pulsed laser ablation method in water as a the liquid environment. In this work, the effect of aging on the structure and optical properties of TiO₂ NPs have been investigated. XRD data reveals that these nanoparticles possessed the orthorhombic brookite structure but with aging the rutile phase (the stable phase) TiO₂ nanoparticles appear in the medium. The excitonic absorption peak of samples immediately after ablation was occurred in wavelength <200 nm and shifted to about 300 nm after a week. Size of nanoparticles increased and their bandgap energy decreased. Result show that aging is a strong effect which may change TiO₂ nanoparticles to rutile stable phase in a week.

Open Access This article is distributed under the terms of the Creative Commons Attribution 4.0 International License (<http://creativecommons.org/licenses/by/4.0/>), which permits unrestricted use, distribution, and reproduction in any medium, provided you give appropriate credit to the original author(s) and the source, provide a link to the Creative Commons license, and indicate if changes were made.

References

1. Dwivedi, N., Kumar, S., Malik, H.K.: Role of ex-situ oxygen plasma treatments on the mechanical and optical properties of diamond-like carbon thin films. *Mater. Chem. Phys.* **134**, 7–12 (2012)
2. Dwivedi, N., Malik, H.K., Rauthan, C.M.S., Panwar, O.S.: Correlation of sp³ and sp² fraction of carbon with electrical, optical and nano-mechanical properties of argon-diluted diamond-like carbon films. *Appl. Surf. Sci.* **257**, 6804–6810 (2011)
3. Singh, O., Dahiya, P., Malik, H.K., Kumar, P., Singh, V.: Investigation of titanium nitride thin films treated in hot cathode arc discharge plasma system. *Appl. Sci. Lett.* **2**, 37–41 (2016)
4. Dwivedi, N., Kumar, S., Malik, H.K.: Strange hardness characteristic of hydrogenated diamond-like carbon thin film by plasma enhanced chemical vapor deposition process. *Appl. Phys. Lett.* **102**, 011917 (2013)
5. Dwivedi, N., Kumar, S., David Carey, J., Tripathi, R.K., Malik, H.K., Dalai, M.K.: Influence of silver incorporation on the structural and electrical properties of diamond-like carbon thin films. *Appl. Mater. Interfaces* **5**, 2725–2732 (2013)
6. Baker, C., Pradhan, A., Pakstis, L., Pochan, D.J., Shah, I.: Synthesis and antibacterial properties of silver nanoparticles. *J. Nanosci. Nanotechnol.* **5**, 244–249 (2005)
7. Pyatenko, A., Shimokawa, K., Yamaguchi, M., Nishimura, O., Suzuki, M.: Synthesis of silver nanoparticles by laser ablation in pure water. *Appl. Phys. A* **79**, 803–806 (2004)
8. Lundqvist, M.J., Nilsing, M., Persson, P., Lunell, S.: DFT study of bare and dye-sensitized TiO₂ clusters and nanocrystals. *Int. J. Quantum Chem.* **106**, 3214–3234 (2006)
9. Subramanian, V., Karki, A., Gnanasekar, K.I., Eddy, F.P., Rambabu, B.: Nanocrystalline TiO₂ (anatase) for Li-ion batteries. *Power Sources* **159**, 186–192 (2006)
10. Li, G., Li, L., Boerio-Goates, J., Woodfield, B.: High purity anatase TiO₂ nanocrystals: near room-temperature synthesis, grain growth kinetics, and surface hydration chemistry. *J. Am. Chem. Soc.* **127**, 8659–8666 (2005)
11. Ahmadi, M., Ghasemi, M., Hashemipour, H.: Study of different parameters in TiO₂ nanoparticles formation. *Mater. Sci. Eng* **5**, 87–93 (2011)
12. Shahani, S., Askari, M., Sadrandahza, S.: Gel–sol synthesis and aging effect on highly crystalline anatase nanopowder. *Bull. Mater. Sci.* **34**, 1189–1195 (2011)
13. Mahoney, L., Rasalingam, S.H., Wu, C.H., Peng, R., Koodali, R.: Aging dependent phase transformation of mesostructured titanium dioxide nanomaterials prepared by evaporation-induced self-assembly process: implications for solar hydrogen production. *AIMS. Mater. Sci.* **2**, 230–242 (2015)
14. Menendez, A., Chichkov, N.B., Barcikowski, S.: Influence of water temperature on the hydrodynamic diameter of gold nanoparticles from laser ablation. *J. Phys. Chem. C* **114**, 2499–2504 (2010)
15. Singh, S.C., Swarnkar, R.K., Gopal, R.: Synthesis of titanium dioxide nanomaterial by pulsed laser ablation in water. *J. Nanosci. Nanotechnol.* **9**, 5367–5371 (2009)
16. Hong, S.M., Lee, S., Jung, H.J., Yu, Y., Shin, J., Kwon, K.Y., Choi, M.Y.: Simple preparation of anatase TiO₂ nanoparticles via pulsed laser ablation in liquid. *Bull. Korean Chem* **34**, 279–282 (2013)
17. Kumar, P., Malik, H.K., Asokan, K.: Tuning of optical bandgap and magnetization of C-implanted ZnO thin films. *Europhys. Lett.* **110**, 67006 (2015)
18. Singh, J.S., Malik, H.K., Vermaa, S.S.: DDA simulations of noble metal and alloy nanocubes for tunable optical properties in biological imaging and sensing. *RSC Adv.* **3**, 15427–15434 (2013)
19. Barreca, F., Acacia, N., Barletta, E., Spadaro, D., Curro, G., Neri, F.: Small size TiO₂ nanoparticles prepared by laser ablation in water. *Appl. Surf. Sci.* **256**, 6408–6412 (2010)
20. Di Paola, A., Bellardita, M., Palmisano, L.: Brookite, the least known TiO₂ photocatalyst. *Catalysts* **3**, 36–73 (2013)

